Desalination and Water Treatment
www.deswater.com
43 (2012) 314–322
April
1944-3994/1944-3986
doi: 10.1080/19443994.2012.672215
Taylor & Francis
Taylor & Francis Group

Application of osmotic backwashing in forward osmosis: mechanisms and factors involved

Changwoo Kim, Sangyoup Lee, Seungkwan Hong*

School of Civil, Environmental & Architectural Engineering, Korea University, 1,5-ka, Anam-Dong, Sungbuk-Gu, Seoul 136-713, Republic of Korea
Tel. +82 2 3290 3322; Fax: +82 2 928 7656; email: skhong21@korea.ac.kr

Received 25 December 2011; Accepted 10 February 2012

ABSTRACT

Feasibility of osmotic backwashing for cleaning fouled membranes during forward osmosis (FO) process was investigated focusing on the mechanisms and factors involved. Alginate and humic acids were used as model organic foulants; and colloidal silica particles with different sizes were used as model inorganic particulate foulants. Results showed that noticeable flux recovery was achieved by osmotic backwashing through the instantaneous replacement of the draw solution with the dilute solution that has much less osmotic pressure than that of the feed solution. The switch of water flow direction through the membrane from feed-to-draw to draw-to-feed allows the effective detachment of foulants from the membrane surface. It was found that the efficiency of osmotic backwashing was affected by several factors including foulant type, membrane orientation and backwashing conditions (i.e. initial flux and duration). In addition, concentration polarization was found to play an important role in determining fouling behaviour, and thus, the osmotic backwashing efficiency.

Keywords: Forward osmosis (FO); Osmotic backwashing; Organic fouling; Particle fouling; Concentration polarization

1. Introduction

A worldwide demand for reverse osmosis (RO) technology in seawater desalination, wastewater treatment and water reuse has been rapidly increased [1–3]. However, despite these demands, major drawbacks such as high energy consumption and inevitable fouling problem in RO processes are holding back its further practical applications [4]. As an alternative or supportive to RO technology, forward osmosis (FO) process is recently getting great attention. Unlike pressure-driven membrane process, FO uses chemical potential gradient between feed water and draw solutions with high osmotic pressure. Thus, FO membrane process, depending on separation and reconstitution of draw solutions, has a potential to reduce energy consumption and increase water recovery in many water and wastewater purification processes [5]. However, it has been recently found that FO is not free from membrane fouling, even though fouling mechanisms and factors affecting fouling are different from those involved in RO [6]. Therefore, FO process also requires membrane cleaning for the efficient operation. To date, however, very few studies on FO cleaning methods have been reported in literature. There

*Corresponding author.

are some attempts such as increasing cross-flow velocity and introducing air bubbles in the feed stream [6,7]. These means, however, are not new and not specific for FO process.

Backwashing is a common and effective cleaning method in membrane processes. In most cases, however, backwashing has been mainly applied to MF and UF, but not to NF and RO as these membranes have an asymmetric structure with very small pores [8–11]. Several attempts to utilize backwashing for RO cleaning have been reported in the previous literature. Spiegler and Macleish described the first direct osmotic backwashing idea in RO [12]. Semiat et al. investigated osmotic backwashing for RO with stopping pump or reducing the pressure [13–18]. Recently, Liberman's group injected the high salinity solution in feed solution line for osmotic backwashing with online operation [19–22]. However, the application of backwashing in FO process is rather scarce even though backwashing can be a promising method for FO cleaning as the instantaneous switch of permeate direction is possible in FO process [23–25].

In this study, the efficiency of osmotic backwashing in FO process has been systemically investigated focusing on the mechanisms and factors involved. Osmotic backwashing was applied to clean FO membranes fouled by organic and inorganic foulants. Various backwashing conditions under two different membrane orientations were also studied for better cleaning efficiency.

2. Material and methods

2.1. FO system

FO membrane cell was a flat-and-frame design with a rectangular channel on each side of membrane. It had a dimension of 7.7 cm length, 2.6 cm width, and 0.3 cm depth, providing an effective membrane area of 20.0 cm^2. Two gear pumps (Ismatec, ISM895) were used to circulate draw and feed solutions in each channel. Flow meters (Blue-white, F-450) were installed for measuring cross-flow. The temperature of draw and feed solutions was maintained at 20°C using chiller (AND, AD-RC08). Change in the weight of draw solution was measured every three minutes using microscale (Cas, Cuw 4200H) connected computer, in which data were collected for the calculation of permeate and backwashing fluxes.

2.2. Osmotic backwashing

The principle of osmotic backwashing employed in this study is schematically presented in Fig. 1. During FO operation as shown in Fig. 1(a), permeate flows from feed-to-draw solutions by the osmotic pressure of draw solution. Thus, foulants in the feed solution are deposited on FO membrane surface. As FO operation continues, draw solution gets diluted and feed solution gets concentrated, leading to decreased effective osmotic pressure difference across the FO membrane. Consequently, permeate flux decreases due to the increase in the total hydraulic resistance as well as the decrease in effective osmotic pressure.

Fig. 1(b) describes the concept of osmotic backwashing. During the osmotic backwashing, the draw solution is replaced by deionized (DI) water. When DI water flows through draw side channel, the osmotic pressure gradients are formed in an opposite direction and permeate (i.e. backwash water) flows from draw (DI water) to feed sides. Therefore, foulants on the membrane surface are possibly detached by this opposite flow and then removed from the channel by the cross-flow.

2.3. FO membrane

The membrane used in the experiments was provided by Hydration Technologies, Inc. (Albany, OR). Fourier transform infrared spectrometer (JASCO, FT-IR 4100) absorption spectrum analysis was first conducted to reveal the chemical composition of FO

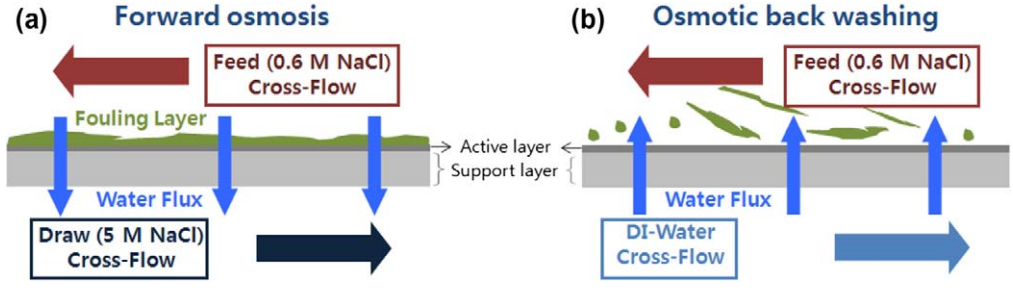

Fig. 1. Principle of osmotic backwashing: (a) normal (FO) operation (permeate flow from feed side to draw side) and (b) osmotic backwashing (permeate flow from draw side (DI water) to feed side).

membranes. The results shown in Fig. 2 indicated that both active and porous layers of the membranes were composed of cellulose acetate with similar chemical structure.

The zeta potential of membrane surface was measured under varying pH conditions, to evaluate the membrane charge using a streaming potential analyzer (SurPASS, Anton Paar GmbH, Graz, Austria). The electrolyte was a 10 mM KCl solution, where the pH was adjusted to be in the range of pH 3–10. Measurements were conducted at a continual pressure in the range of 0–500 mbar with a temperature of 24–25° C. Zeta potential values were calculated from the measured streaming potential using the Helmholtz-Smoluchowski equation with the Fairbrother and Mastin substitution [26]. The results presented in Fig. 3 showed that both sides of the membrane displayed low but constant negative charges throughout the pH range investigated.

Lastly, contact angle measurements were performed with a goniometer (DM 500, Kyowa Interface Science, Japan). Equilibrium contact angle measurements, as described by Marmur [27], were adopted. The equilibrium contact angle was the average of the left and right contact angles. Ten measurements were conducted for each membrane and the reported values are the average of 10 equilibrium contact angles. As shown in Fig. 4, both sides of the membrane had similar hydrophobicity. Based on these characteristics, it can be concluded that both sides of the membrane are quite similar in terms of chemical surface characteristics.

2.4. Model foulants

Alginate and humic acid (HA) were used as model organic foulants to represent common polysaccharides and natural organic matter, respectively. These organic macromolecules have been reported to be the major components of organic fouling found in various membrane filtration processes of surface water, seawater and wastewater effluent [28,29]. Alginate and HA (Sigma-Aldrich, St. Louis, MO) were received in a powder form. The molecular weights of alginate and HA are approximately 12–80 and 1–5 kDa, respectively [30,31].

Two different sizes of silica (SiO_2) particles were used as model inorganic particulate foulants. The sizes of these model particles were reported to be 20 nm (ST-30) and 100 nm (ST-ZL, Nissan Chemical Industries, NY). The size of silica particles was further verified using a particle size analyzer (Mastersizer, Malvern Ins.), and their size distributions are presented in Fig. 5. As shown, an actual average diameter of ST-30 and ST-ZL silica particles were determined to be approximately 24 and 139 nm, respectively.

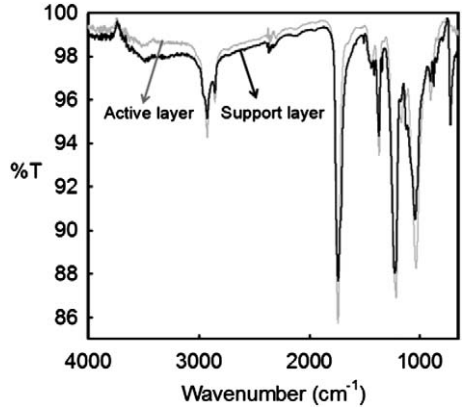

Fig. 2. Fourier transform infrared spectrometer (FT-IR) absorption spectrum analysis of FO membrane (surface of the active layer and support layer of the HTI membrane tested).

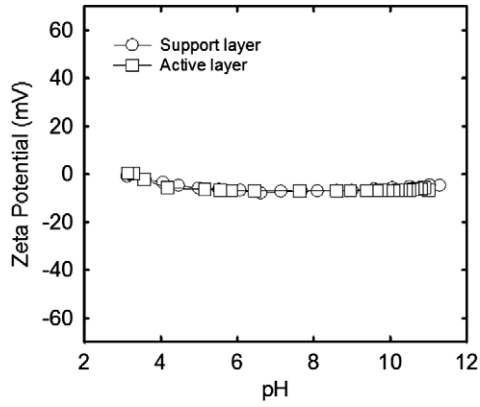

Fig. 3. Membrane surface zeta potential plotted as a function of solution pH at a background electrolyte concentration of 10 mM KCl. Solution temperature was maintained at 25°C.

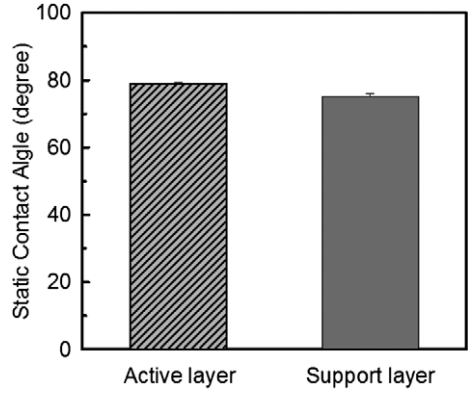

Fig. 4. Contact angle measurements of FO membrane at the solution chemistry employed in this study.

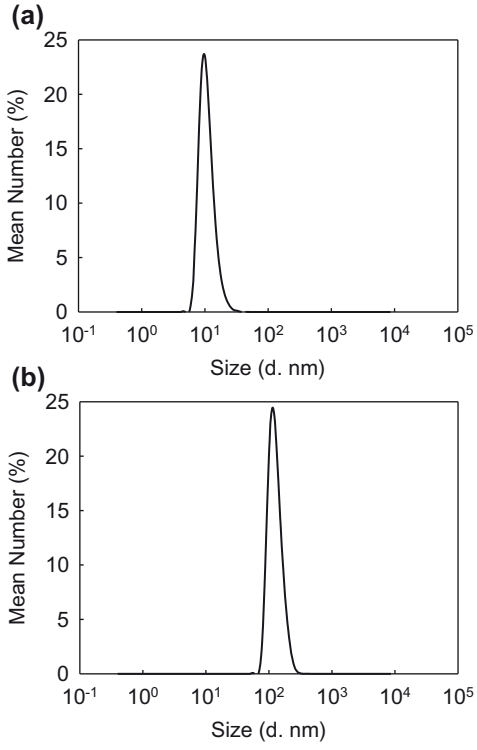

Fig. 5. Size distribution of silica particles used in fouling experiments: (a) 20 nm and (b) 100 nm.

Gravimetric analysis revealed that the densities of 20 and 100 nm particles were 2.1 and 2.3 g/cm^3, respectively. The particles were diluted with DI water (D7429-33, Easy Pure RO system, LabScience, Korea) to be the concentration of 2 g/L. Silica particles were used after sonication (8510E-DTH, Branson Ultrasonic CO., Danbury, CT, USA) for over 10 min to prevent particle aggregation.

2.5. Application of osmotic backwashing to FO process

In order to simulate seawater osmotic pressure, 0.6 M NaCl was used as a feed solution and various foulants (i.e. alginate, HA, and different sizes of SiO_2 particles) were added to this feed solution. 5 M NaCl was used as a draw solution in the active layer faced feed solution (AL-FS) and 3.8 M NaCl in active layer faced draw solution (AL-DS). It may be noted that the reason for the difference in draw solution concentration with respect to membrane orientation is to adjust the initial flux to be the same for both cases. By doing so, the same initial permeation drag force could be applied.

Fouling experiments were conducted as follows. Initial volume of feed and draw solutions was 2.0 L. The cross-flow velocity for both feed and draw solutions was fixed at 8.5 cm/s. Temperature of feed and draw solutions was maintained at 20°C and pH of feed solution was fixed at 7.0. The fouling experiments were continued until 300 mL of permeate was obtained, where noticeable flux decline was observed due to fouling. Then, osmotic backwashing was conducted by simply replacing the draw solution with DI water instantaneously for 30 min. After the osmotic backwashing was performed, DI water was changed to the draw solution used in the previous fouling test and permeate flux was measured under the same operating conditions employed in the fouling experiments. By comparing the permeate flux at the end of fouling experiments to the flux recovered after osmotic backwashing, the cleaning efficiency was determined.

3. Results and discussion

3.1. Baseline experiments

Water permeation in FO process is driven by the osmotic pressure difference between draw and feed solutions. In the common lab-scale FO system, permeate water flows from feed-to-draw side inherently involves the simultaneous concentration and dilution of feed and draw solutions, respectively. This leads to permeate flux decline even at the absence of fouling. Furthermore, at the end of osmotic backwashing, draw solution is slightly mixed with the remaining DI water and feed solution is slightly diluted by the water from backwashing. This also results in flux reduction without fouling. Therefore, baseline experiment (i.e. foulant-free condition) is required prior to fouling and backwashing experiments to compensate inherent flux changes.

During the baseline experiments, 5.0 and 3.8 M NaCl were used as draw solutions in AL-FS and AL-DS, respectively. To simulate the seawater-level osmotic pressure, 0.6 M NaCl was used as a feed solution. The difference in the concentration of the draw solutions in AL-FS and AL-DS modes is to make the initial fluxes of two modes to be the same. The results obtained from the baseline experiments are presented in Fig. 6. As shown, permeate flux was decreasing gradually throughout the entire span of baseline experiments for both modes due to the reasons mentioned above. These baseline flux data were used to correct flux curves obtained from fouling and osmotic backwashing experiments.

3.2. Organic fouling

3.2.1. Alginate

To verify the effect of osmotic backwashing on alginate fouling, fouling and osmotic backwashing

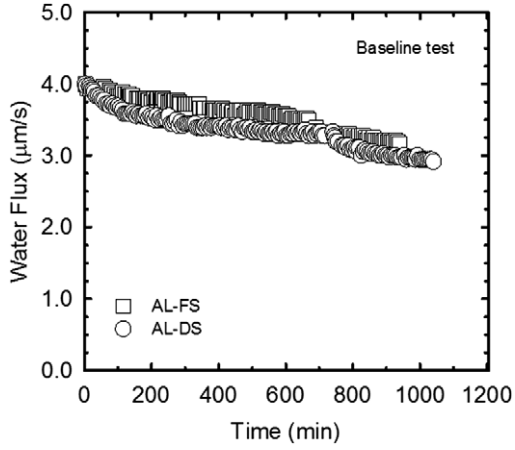

Fig. 6. Flux of baseline experiments in AL-FS and AL-DS.

experiments were conducted with feed solution of 0.6 M NaCl and 200 mg/L alginate. FO membrane used in this study was composed of dense active layer on the top of rough porous layer. Thus, alginate fouling occurred on the active layer of AL-FS mode and porous layer of AL-DS mode, respectively. The flux decline curves obtained during alginate fouling and osmotic backwashing experiments are depicted in Fig. 7(a). In addition, Fig. 7(b) shows the corresponding normalized flux decline and flux recovery in AL-FS and AL-DS modes. Similar flux behaviours were observed in AL-FS and AL-DS, although slightly less flux decline was observed for AL-FS. Permeate flux continuously decreased due to the increase of hydraulic resistance resulted from alginate fouling.

Membrane fouling is generally governed by the coupled influence of chemical and hydrodynamic interactions [32]. It should be noted that chemical properties (i.e. zeta potential, chemical functionality and contact angle) of active and porous layers were almost identical. However, physical properties, typically seen from SEM image, were clearly different as expected. Chemical interactions between foulants and membrane in AL-FS were assumed to be identical to those in AL-DS because of similar chemical membrane characteristics and identical feed solution chemistry. On the other hand, hydrodynamic interactions affecting the extent and degree of membrane fouling can be classified to be permeation drag force resulting from convective flow toward the membrane and shear force caused by cross-flow velocity. In this study, permeation drag force was applied equally in AL-FS and AL-DS modes since the initial water flux was adjusted to be the same. Thus, slightly more flux decline in AL-DS could be attributed to the ineffectiveness to remove alginates captured inside the pores by

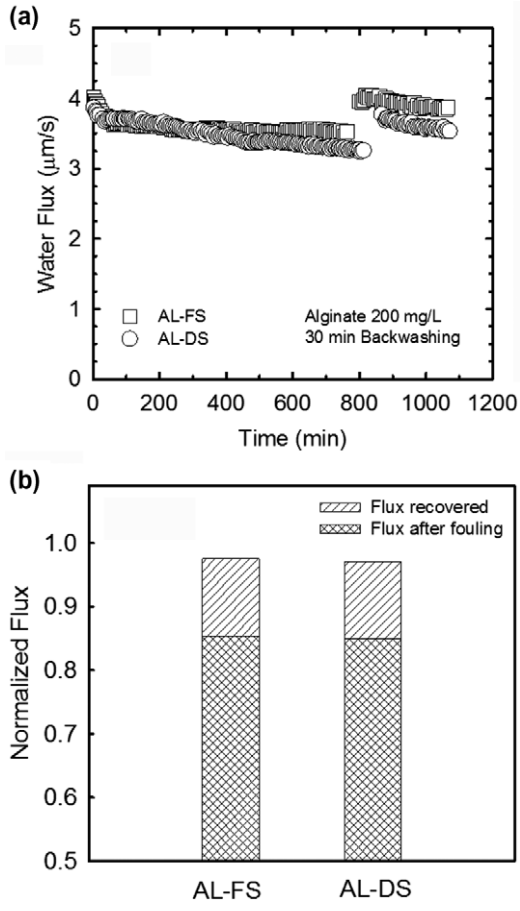

Fig. 7. Fouling and osmotic backwashing experiments with 200 mg/L of alginate: (a) flux decline and recovery plotted as a function of filtration time, and (b) normalized flux decline and flux recovery. Flux curves were corrected by baseline experiments.

cross-flow. In other words, less fouling was observed for AL-FS, since alginate was removed more easily by shear force caused by cross-flow [33].

During osmotic backwashing, draw solution was replaced by DI water. As a result, permeation drag force was vanished instantaneously. Then, water moved oppositely from draw-to-feed side, and thus, the alginate fouling layer was disrupted, detached and removed. As shown in Fig. 7, osmotic backwashing was quite effective to recover the flux declined during alginate fouling and there was no significant difference between AL-FS and AL-DS modes in terms of the efficiency of flux recovery. The reasons for effective flux recovery can be interpreted by fouling mechanism and hydrophilic property of alginate. Due to its relatively hydrophilic nature, alginate was less chemically interacted with FO membrane surface, and thus, simply accumulated on the active layer of AL-FS and inside porous layer of AL-DS. When osmotic backwashing was performed, alginate was removed

more easily by reverse water flow through the FO membrane.

3.2.2. Humic acid

Feed solution of 0.6 M NaCl containing 200 mg/L HA was used to investigate the effect of osmotic backwashing on HA fouling. The flux decline curves obtained during HA fouling and osmotic backwashing experiments are presented in Fig. 8(a) as a function of filtration time. Fig. 8(b) also shows normalized flux decline and normalized flux recovery for HA fouling and osmotic backwashing, respectively. As shown, more severe flux decline was observed in AL-DS. As mentioned earlier, this difference in flux decline between AL-FS and AL-DS could be attributed mainly to the effect of shear force applied in two modes. In AL-FS mode, permeate flux declined much less, indicating that HA was effectively removed by shear force. In AL-DS, on the other hand, HA captured in porous structure of FO membrane was not removed effectively by cross-flow, resulting in severe permeate flux decline. Furthermore, hydrophobic nature of HA enhanced chemical interaction with FO membrane surface and possibly increased their attachments to the inside pores of AL-DS.

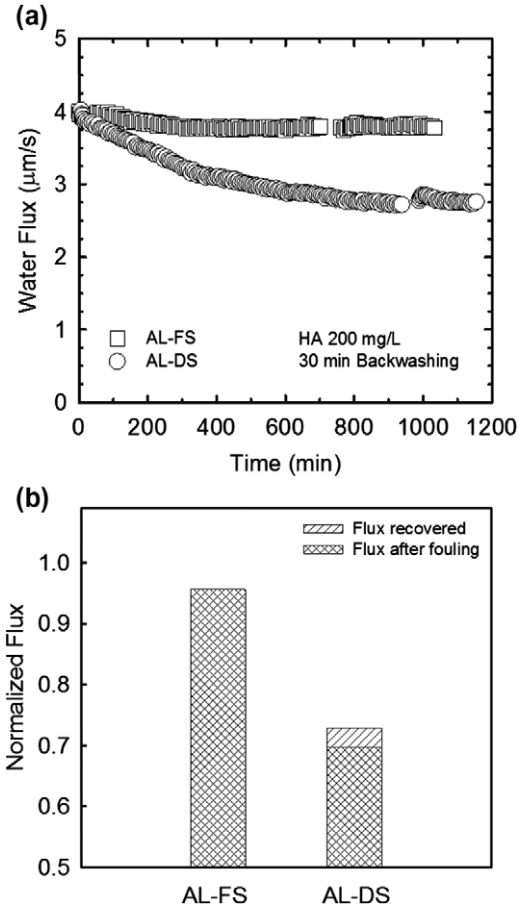

Fig. 8. Fouling and osmotic backwashing experiments with 200 mg/L of HA: (a) flux decline and recovery as plotted as a function of filtration time and (b) normalized flux decline and flux recovery. Flux curves were corrected by baseline experiments.

When osmotic backwashing was performed, the flux recovery of HA experiments was found to much less compared to that of alginate experiments, particularly in AL-DS mode, implying that the osmotic backwashing efficiency is greatly affected by the type of foulants. It should be noted that the efficiency of osmotic backwashing was not accurately measured for AL-FS mode, since permeate flux decline was not severe. HA exhibits relatively greater hydrophobicity compared to alginate. Thus, it is more difficult to remove HA by osmotic backwashing. More systematic studies are needed in the future to optimize the backwashing efficiency when various organic foulants are present simultaneously in the feed water.

3.3. Particulate fouling

Feed solution of 0.6 M NaCl containing 2 g/L of 20 and 100 nm silica (SiO_2) particles was utilized to investigate the effect of osmotic backwashing on particulate fouling. The results are described schematically in Figs. 9 and 10 for 20 and 100 nm SiO_2 particles, respectively. In case of experiments with smaller particles (20 nm), flux decline in AL-DS was more severe than AL-FS, as shown in Fig. 9. This observation was attributed to the difference in effectiveness of shear flow in two modes, similar to organic fouling, particularly to HA fouling. The shear force exerted by cross-flow was not able to effectively remove small colloidal particles entrapped inside pores of AL-DS. However, a noticeable flux recovery in AL-DS was found after osmotic backwashing, although flux was not completely recovered. It may be noted that particle concentrations used in this study were relatively large compared to typical seawater desalination. Thus, osmotic backwashing may be more effective and feasible in real applications. Lastly, it should be mentioned that the efficiency of osmotic backwashing was not accurately assessed for AL-FS, due to much less flux decline by silica fouling.

In contrast to 20 nm particle, fouling behaviours of 100 nm SiO_2 particles were almost the same in AL-FS and AL-DS modes. As presented in Fig. 10, permeate flux declined rapidly and significantly for both modes. The flux decline rates of AL-FS and AL-DS were identical, indicating severe particle fouling occurred in

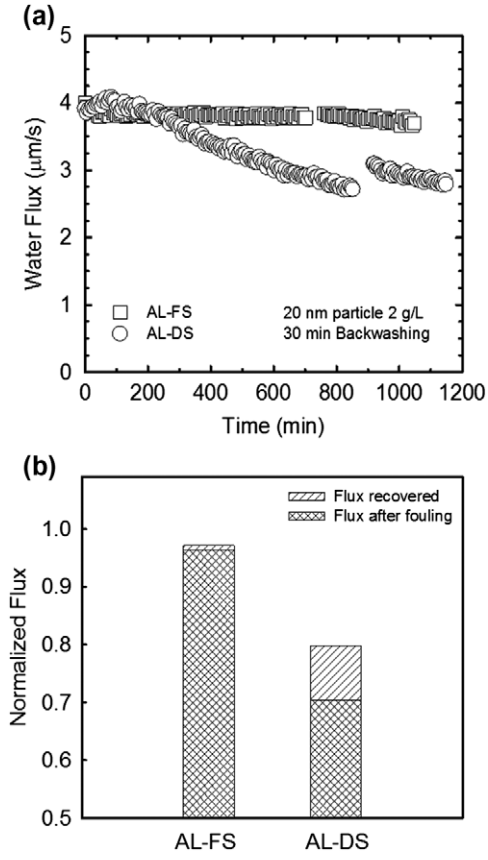

Fig. 9. Fouling and osmotic backwashing experiments with 2 g/L of 20 nm silica particles: (a) flux decline and recovery as plotted as a function of filtration time, and (b) normalized flux decline and flux recovery. Flux curves were corrected by baseline experiments.

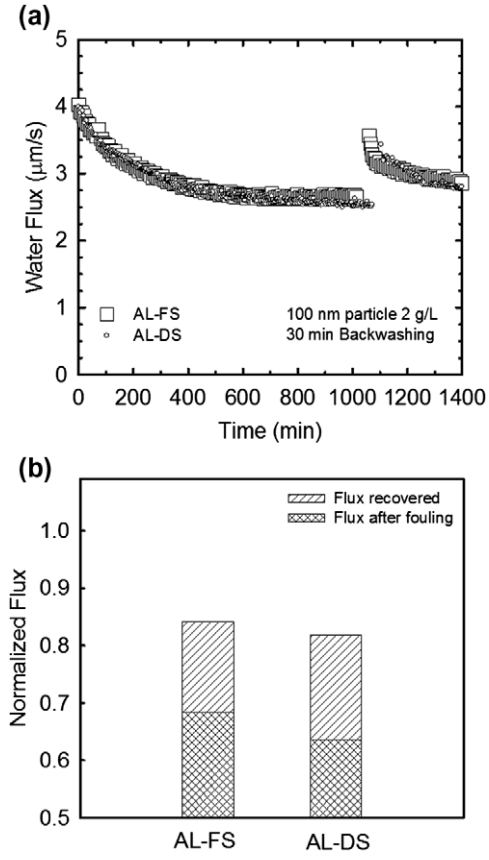

Fig. 10. Fouling and osmotic backwashing experiments with 2 g/L of 100 nm silica particles: (a) flux decline and recovery as plotted as a function of filtration time and (b) normalized flux decline and flux recovery. Flux curves were corrected by baseline experiments.

both modes. In addition, the degree of flux decline is most severe than other fouling cases explored in this study (i.e. alginate, HAs, and 20 nm particles). These findings can be explained by cake-enhanced osmotic pressure (CEOP) at the presence of particle cake layer formed by large silica colloidal particles [30]. Furthermore, large colloids were less removed from the membrane surface due to small diffusion coefficient of large particles [34]. However, over 85% of flux declined during fouling experiments was recovered by osmotic backwashing. This means that the backwashing water effectively diluted the salt concentration within colloidal cake layer and, hence, decreased significantly CEOP, leading to successful flux recovery.

Fouling and flux recovery behaviours of the 100 nm SiO_2 particles were quite different from those of 20 nm particles. In typical FO membranes, the reverse diffusion of draw solutes occurs from draw solution to feed water. Larger particles such as 100 nm silica typically form a thick cake layer on the membrane surface mainly due to smaller transport back to feed water. Furthermore, salts entrapped within such cake layer are hard to diffuse. When draw solutes are reversely diffused to feed water, salt concentration at the membrane surface dramatically increases further due to CEOP [35]. As a result, permeate flux of AL-FS declined markedly, even similar to that of AL-DS.

3.4. Backwashing water flux

When osmotic backwashing experiments were performed, backwashing water flux was monitored every 3 min. Fig. 11 shows backwashing water flux under baseline and fouling conditions. It is very interesting to observe higher initial backwashing water flux with fouling experiments, compared to baseline tests, for both AL-FS and AL-DS. This result can be attributed to the change of concentration polarization (CP) profile due to fouling layer formation. Fouling layer

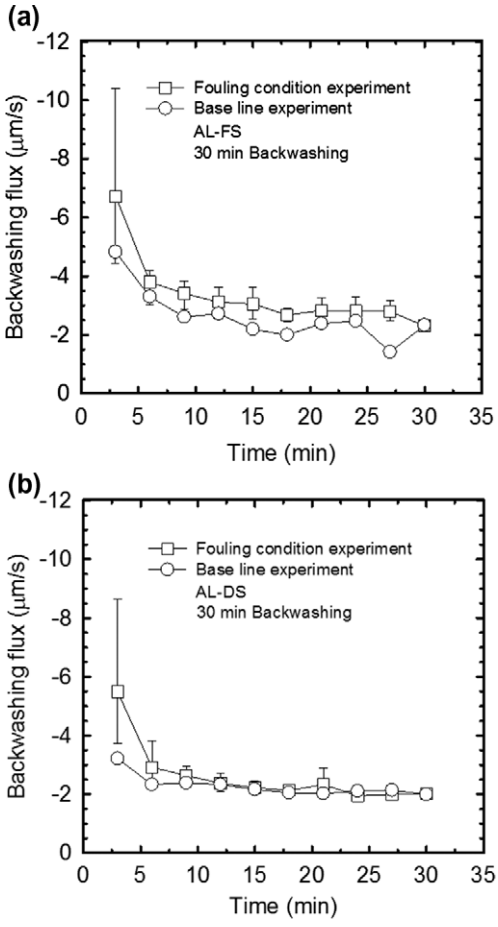

Fig. 11. Backwashing water flux under baseline and fouling conditions: (a) AL-FS and (b) AL-DS. Note that negative flux values indicate reverse flow direction.

formed on the surface of FO membrane hinders back transport of salts, and thus, enhances CP. When osmotic backwashing is performed, the draw solution is replaced by DI water; and higher salt concentration in the feed water side due to enhanced CP draws more DI water through FO membrane, leading to higher initial backwash water flux. Therefore, to increase the efficiency of osmotic backwashing, the duration and time interval need to be carefully optimized.

4. Conclusion

In this study, osmotic backwashing was applied and evaluated to control organic and particle fouling in FO membrane process using organic (i.e. alginate and HAs) and inorganic (i.e. SiO_2 particles) foulants. It was clearly demonstrated that fouling behaviour and flux recovery by osmotic backwashing were significantly influenced by the type of foulants and membrane orientation. Generally, less fouling was observed for AL-FS mode, typical FO process, compared to AL-DS mode. Severe fouling in AL-DS can be explained by the ineffectiveness of shear force exerted by cross-flow to remove foulants entrapped in porous structure of support layer in FO membrane. Osmotic backwashing was able to effectively restore the flux, although flux recovery was not completely achieved. However, considering the fact that this study was conducted under accelerated fouling conditions with higher foulants' concentration, it is concluded that osmotic backwashing could be a promising method to clean fouled membranes during FO process. Lastly, it should be mentioned that, since fouling mechanisms of FO membrane process are more complex and not clearly known, more systematic studies are needed to optimize the backwashing efficiency.

Acknowledgements

This research was supported by WCU programme through the National Research Foundation of Korea founded by the ministry of Education, Science and Technology (R33-10046).

References

[1] T.Y. Cath, A.E. Childress, M. Elimelech, Forward osmosis: principles, applications, and recent developments, J. Membr. Sci. 281 (2006) 70–87.
[2] M.I. Dova, K.B. Petrotos, H.N. Lazarides, On the direct osmotic concentration of liquid foods. Part I. Impact of process parameters on process performance, J. Food Eng. 78 (2007) 422–430.
[3] B. Jiao, A. Cassano, E. Drioli, Recent advances on membrane processes for the concentration of fruit juices: A review, J. Food Eng. 63 (2004) 303–324.
[4] H.Y. Ng, W. Tang, W.S. Wong, Performance of forward (direct) osmosis process: Membrane structure and transport phenomenon, Environ. Sci. Technol. 40 (2006) 2408–2413.
[5] Y. Xu, X. Peng, C.Y. Tang, Q.S. Fu, S. Nie, Effect of draw solution concentration and operating conditions on forward osmosis and pressure retarded osmosis performance in a spiral wound module, J. Membr. Sci. 348 (2010) 298–309.
[6] S. Lee, C. Boo, M. Elimelech, S. Hong, Comparison of fouling behavior in forward osmosis (FO) and reverse osmosis (RO), J. Membr. Sci. 365 (2010) 34–39.
[7] B. Mi, M. Elimelech, Organic fouling of forward osmosis membranes: Fouling reversibility and cleaning without chemical reagents, J. Membr. Sci. 348 (2010) 337–345.
[8] K.N. Bourgeous, J.L. Darby, G. Tchobanoglous, Ultrafiltration of wastewater: Effects of particles, mode of operation, and backwash effectiveness, Water Res. 35 (2001) 77–90.
[9] S. Hong, P. Krishna, C. Hobbs, D. Kim, J. Cho, Variations in backwash efficiency during colloidal filtration of hollow-fiber microfiltration membranes, Desalination 173 (2005) 257–268.
[10] X. Shengji, L. Xing, Y. Ji, D. Bingzhi, Y. Juanjuan, Application of membrane techniques to produce drinking water in China, Desalination 222 (2008) 497–501.
[11] A. Sagiv, R. Semiat, Modeling of backwash cleaning methods for RO membranes, Desalination 261 (2010) 338–346.
[12] K.S. Spiegler, J.H. Macleish, Molecular (osmotic and electro-osmotic) backwash of cellulose acetate hyperfiltration membranes, J. Membr. Sci. 8 (1981) 173–192.

[13] M. Ando, K. Ishii, S. Ishihara, Running method and treatment system for spiral wound membrane element and spiral wound membrane module, EP 1170053 A1 20020109, 2002.
[14] M. Ando, T. Watanabe, H. Yoshikawa, Treatment system having spiral membrane element and method for operating the treatment system, EP 1323461 A2 20030703, 2003.
[15] A. Sagiv, R. Semiat, Backwash of RO spiral wound membranes, Desalination 179 (2005) 1–9.
[16] N. Avrham, C. Dosoretz, R. Semiat, Osmotic backwash process in RO membranes, Desalination 199 (2006) 387–389.
[17] A. Sagiv, N. Avrham, C.G. Dosoretz, R. Semiat, Osmotic backwash mechanism of reverse osmosis membranes, J. Membr. Sci. 322 (2008) 225–233.
[18] A. Sagiv, R. Semiat, Parameters affecting backwash variables of RO membranes, Desalination 261 (2010) 347–353.
[19] B. Liberman, Direct osmosis cleaning, Patent application, WO 2004/062774, 2004 and US Patent Application 20070246425, 2007.
[20] I. Liberman, RO membrane cleaning method, PCT, WO 2005/123232 A2 0181497, 2005.
[21] B. Liberman, I. Liberman, RO membrane cleaning – replacing membrane CIP by direct osmosis cleaning, Desalin. Water Reuse 15 (2005) 28–32.
[22] J.J. Qin, M.H. Oo, K.A. Kekre, B. Liberman, Development of novel backwash cleaning technique for reverse osmosis in reclamation of secondary effluent, J. Membr. Sci. 346 (2010) 8–14.
[23] R.W. Holloway, A.E. Childress, K.E. Dennett, T.Y. Cath, Forward osmosis for concentration of anaerobic digester centrate, Water Res. 41 (2007) 4005–4014.
[24] C.R. Martinetti, A.E. Childress, T.Y. Cath, High recovery of concentrated RO brines using forward osmosis and membrane distillation, J. Membr. Sci. 331 (2009) 31–39.
[25] A. Achilli, T.Y. Cath, E.A. Marchand, A.E. Childress, The forward osmosis membrane bioreactor: A low fouling alternative to MBR processes, Desalination 239 (2009) 10–21.
[26] S.S. Deshrnukh, A.E. Childress, Zeta potential of commercial RO membranes: Influence of source water type and chemistry, Desalination 140 (2001) 87–95.
[27] A. Marmur, Equilibrium contact angles: Theory and measurement, Colloid Surf. A 116 (1996) 55–61.
[28] G.T. Grant, E.R. Morris, D.A. Rees, J.C. Smith, D. Thom, Biological interaction between polysaccharides and divalent cations: The egg-box model, FEBS Lett. 32 (1973) 195–198.
[29] H. Ma, H.E. Allen, Y. Yin, Characterization of isolated fractions of dissolved organic matter from natural waters and a wastewater effluent, Water Res. 35 (2001) 985–996.
[30] S. Lee, J. Cho, M. Elimelech, Combined influence of natural organic matter (NOM) and colloidal particles on nanofiltration membrane fouling, J. Membr. Sci. 262 (2005) 27–41.
[31] C.S. Uyguner, M. Bekbolet, A comparative study on the photocatalytic degradation of humic substances of various origins, Desalination 176 (2005) 167–176.
[32] A. Seidel, M. Elimelech, Coupling between chemical and physical interactions in natural organic matter (NOM) fouling of nanofiltration membranes: Implications for fouling control, J. Membr. Sci. 203 (2002) 245–255.
[33] B. Mi, M. Elimelech, Chemical and physical aspects of organic fouling of forward osmosis membranes, J. Membr. Sci. 320 (2008) 292–302.
[34] P. Bacchin, P. Aimar, R.W. Field, Critical and sustainable fluxes: Theory, experiments and applications, J. Membr. Sci. 281 (2006) 42–69.
[35] C. Boo, S. Lee, M. Elimelech, Z. Meng, S. Hong, Colloidal fouling in forward osmosis: Role of reverse salt diffusion, J. Membr. Sci. 390–391 (2012) 277–284.